Chemical Engineering Journal 353 (2018) 533–541

Contents lists available at ScienceDirect

Chemical Engineering Journal

journal homepage: www.elsevier.com/locate/cej

Performances and mechanisms of efficient degradation of atrazine using peroxymonosulfate and ferrate as oxidants

Shaohua Wu[a,1], Huiru Li[a,1], Xiang Li[a,1], Huijun He[a,*], Chunping Yang[a,b,*]

[a] College of Environmental Science and Engineering, Hunan University and Key Laboratory of Environmental Biology and Pollution Control (Hunan University), Ministry of Education, Changsha, Hunan 410082, China

[b] Zhejiang Provincial Key Laboratory of Waste Treatment and Recycling, College of Environmental Science and Engineering, Zhejiang Gongshang University, Hangzhou, Zhejiang 310018, China

HIGHLIGHTS

- Novel pathways of atrazine degradation by Fe(VI)/PMS were proposed.
- Sulfate radical was the predominant radical responsible for atrazine degradation.
- Maghemite particles resulted from Fe(VI) reduction could activate PMS.
- Fe(VI)/PMS process efficiently degraded atrazine.

ARTICLE INFO

Keywords:
Peroxymonosulfate
Ferrate
Atrazine
Intermediates
Advanced oxidation process

ABSTRACT

In this study, the degradation efficiencies and mechanisms of atrazine, a recalcitrant herbicide, were thoroughly investigated using ferrate (Fe(VI))/peroxymonosulfate (PMS) process. In comparison with Fe(VI) or PMS alone, Fe(VI)/PMS process significantly enhanced the degradation of atrazine, and its degradation efficiency was higher than that of Fe(VI)/persulfate or Fe(VI)/H_2O_2 process at pH 6.0. Complete degradation of atrazine at an initial concentration of 46.5 μM could be achieved within 20 min at initial concentrations of 6.0 mM Fe(VI), 5.0 mM PMS, pH 6.0, and 25 °C. Fe(VI)/PMS could efficiently degrade atrazine within a wide range of pH values (5–9). NOM concentration lower than 4.0 mg/L was favorable for atrazine degradation. Results of electron spin resonance and quenching studies indicated that both hydroxyl radical and sulfate radical were generated in the Fe(VI)/PMS process, while sulfate radical was the dominant reactive radical responsible for atrazine degradation. The mechanisms of PMS activation were elucidated on the basis of the results of XRD and XPS. In addition, fourteen intermediates from atrazine degradation were identified by LC/MS/MS, and consequently pathways for the degradation were proposed.

1. Introduction

Atrazine is one of the most widely used herbicides for the control of broadleaf weeds in agriculture [1,2]. Atrazine is frequently detected in ground water and surface water (e.g., Suquía River basin, Argentina) due to its moderate aqueous solubility, high mobility and long half-life (30–100 days) [3], and the detected concentration is above the maximum permissible limit (0.1 μg/L) established by the European Union for drinking water [4]. Atrazine can also act as an endocrine disruptor that induces the complete feminization of amphibians such as *Xenopus laevis* [5], posing a potential risk to human health. Moreover, atrazine can cause carcinogenic effects even at a low dose [6]. Unfortunately, numerous methods including nanofiltration [7], adsorption [8,9], coagulation [10], and biodegradation [11–13] cannot effectively remove atrazine from water, and thus higher removal efficiencies for atrazine are urgently needed.

In recent years, advanced oxidation processes (AOPs), especially those based on sulfate radicals ($SO_4^{\cdot -}$) have received close attention for the degradation of organic pollutants [14–16]. Compared with hydroxyl radicals (·OH), $SO_4^{\cdot -}$ has a higher redox potential (2.5–3.1 V) and selectivity, as well as a longer half-life (30–40 μs) [17,18]. It has been reported that $SO_4^{\cdot -}$, as a strong one-electron oxidant, is more

* Corresponding authors at: College of Environmental Science and Engineering, Hunan University, Changsha, Hunan 410082, China.
E-mail addresses: hehuijun@hnu.edu.cn (H. He), yangc@hnu.edu.cn (C. Yang).

[1] These authors contribute to this paper equally.

https://doi.org/10.1016/j.cej.2018.06.133
Received 4 February 2018; Received in revised form 7 June 2018; Accepted 20 June 2018
Available online 21 June 2018

inclined to attack organic compounds with unsaturated and aromatic electrons [14]. As a result, $SO_4^{\cdot -}$-based AOPs will be more efficient in natural water matrices for the degradation of target contaminants. $SO_4^{\cdot -}$ can be generated from the activation of persulfate (PS) and peroxymonosulfate (PMS) using ultraviolet (UV) light [19], heat [20], microwave [21], ultrasound [22], base [23], and transition metals [24,25]. Previous studies have reported that the lower unoccupied molecular orbital of PMS has a lower energy than that of PS or hydrogen peroxide (H_2O_2) [26,27], which suggests that PMS accepts electrons more readily. In addition, PMS appears to be more easily activated due to its asymmetric structure. Although cobalt (Co) is considered as the most efficient PMS activator, its leaching will cause secondary pollution [28]. Other iron-based activators such as ferrous ion (Fe(II)) and nanoscale zero-valent iron for the degradation of atrazine have received much attention due to their low cost, low toxicity and environmental friendliness [10,24]. Nevertheless, the rapid consumption of $SO_4^{\cdot -}$ by excess Fe(II) and the slow conversion from ferric iron (Fe(III)) to Fe(II) limit their practical application.

Ferrate (Fe(VI)) has emerged as an environmentally friendly oxidant and coagulant for the elimination of a wide range of contaminants [29–31], with a redox potential of 0.72–2.20 V (Eqs. (1) and (2)). Meanwhile, its use does not produce undesirable disinfection by-products [32]. Previous studies have shown that Fe(VI) preferably reacts with electron-rich organic pollutants via one-electron or oxygen transfer mechanisms [33,34]. For example, Fe(VI) can oxidize atrazine by attacking alkyl chain moieties [34]. In recent years, the combination of Fe(VI) and other chemicals such as H_2O_2 and sulfite has been regarded as an innovative chemical oxidation technology for the treatment of organic pollutants [35–37]. Fe(VI)/ozone process can also effectively inhibit the formation of bromate, compared with ozone oxidation [38]. Thus, the combined use of Fe(VI) and PMS for the degradation of organic pollutants is feasible. Feng et al. [39] showed that fluoroquinolones could be effectively oxidized by the Fe(VI)/PMS process. However, to the best of our knowledge, the degradation efficiencies and mechanisms of the Fe(VI)/PMS process for the degradation of organic pollutants have not been systematically investigated. Moreover, the predominant reactive species (·OH or $SO_4^{\cdot -}$) during the Fe(VI)/PMS process have been not identified.

$$FeO_4^{2-} + 8H^+ + 2e^- \rightarrow Fe^{3+} + 4H_2O(E^0 = +2.\ 20V) \quad (1)$$

$$FeO_4^{2-} + 4H_2\ O + 3e^- \rightarrow Fe(OH)_3 + 5OH^-(E^0 = +0.72V) \quad (2)$$

In the present study, we propose the combined use of PMS and Fe(VI) for the degradation of atrazine. Our hypothesis is that Fe(VI) can induce the decomposition of PMS to generate reactive species, resulting in an efficient degradation of atrazine. Iron (III) oxides/hydroxides particles could be formed from Fe(VI) reduction after adding Fe(VI) into the solution [29,40], which played a key role in activating PMS as confirmed by Ji et al. [41]. Therefore, we tested this hypothesis by exploring the mechanism of PMS activation using electron spin resonance (ESR) and quenching studies and analyzing the formed solids resulting from Fe(VI) reduction by X-ray diffraction (XRD) and X-ray photoelectron spectroscopy (XPS). The effects of the operational parameters (Fe(VI) and PMS doses, pH, temperature, and NOM) on atrazine degradation were evaluated. The degradation pathways of atrazine by Fe(VI)/PMS were proposed. In addition, the application of the Fe(VI)/PMS process in real water was assessed.

2. Materials and methods

2.1. Materials

Peroxymonosulfate triple salts (PMS, ≥47% $KHSO_5$ basis), and atrazine (> 97.0%) were purchased from Sigma-Aldrich. Potassium ferrate (> 98.0%) was obtained from Shanghai Macklin Biochemical Co., Ltd. 5, 5-Dimethyl-1-pyrroline N-oxide (DMPO, > 97.0%), methanol (MeOH), persulfate, humic acid (used as natural organic matter (NOM)), nitrobenzene, *tert*-butanol (TBA), sodium thiosulfate, phenol, and hydrogen peroxide were of analytical grade and purchased from Sinopharm Chemical Reagent Co., Ltd. All solutions were prepared in Milli-Q water (> 18 MΩ cm) from a Milli-Q system.

2.2. Characterization

The crystallinity of the Fe(VI) resultant particles after reaction was characterized by X-ray diffraction (XRD, Rigaku D/MAX-RB) with Cu Kα radiation. X-ray photoelectron spectroscopy (XPS, Thermo Fisher-VG Scientific) was performed with monochromatic Al Kα radiation. The zeta potential of Fe(VI) in solution was measured at different pH values using a zeta potential meter (Zetasizer Nano-ZS90, Malvern).

2.3. Preparation of atrazine solutions in real water

Four different water samples were collected, including Milli-Q water, tap water, and samples from the Xiangjiang River, and Taozi Lake (Changsha, China). All samples were filtered through a 0.45 μm membrane filter. Atrazine solutions in different water samples were prepared at a concentration of 46.5 μM by magnetic stirring for 48 h and stored at 4 °C.

2.4. Experimental procedures

Batch experiments were conducted in 250 mL conical flasks with a water-bath shaker (150 rpm). Typically, 100 mL of 46.5 μM atrazine solution was prepared. Unless otherwise stated, the solution pH was adjusted to 6.0 ± 0.1 with 0.1 M NaOH or H_2SO_4, due to the high reactivity of $HFeO_4^-$ with atrazine [34]. The desired amount of PMS was added to the above solution, and subsequently 49.5 mg (equivalent to 2.5 mM) Fe(VI) was added to initiate the reaction. At defined time intervals, 1 mL samples were collected and quenched by adding 25 μL of 1.0 M sodium thiosulfate. In addition, the effects of the dosages of PMS and Fe(VI), NOM, pH, and temperature on atrazine degradation were evaluated. Quenching experiments were carried out to determine the contributions of the reactive species, using TBA, MeOH, and phenol as radical scavengers. ESR spectra were measured on a JES FA200 spectrometer, and the settings used are available in Text S1. All experiments were conducted in triplicate, and the standard deviations were shown.

2.5. Analytical methods

Atrazine and nitrobenzene in samples were measured by high-performance liquid chromatography (HPLC, Agilent, USA) using a ZORBAX SB-C18 column (4.6 × 250 mm, 5 μm) equipped with a UV–vis detector at 230 nm and 263 nm, respectively. The mobile phase for atrazine was composed of methanol, water and acetonitrile (60/30/10, v/v/v) at a flow rate of 1 mL/min, and column temperature was set at 40 °C. The mobile phase for nitrobenzene was composed of methanol and water (60/40, v/v) at a flow rate of 1 mL/min, and column temperature was set at 25 °C. Injection volume was 20 μL. Total organic carbon (TOC) was determined by a TOC-5050A analyzer (Shimadzu, Japan). The concentrations of Fe(II) and Fe(III) were detected at 510 nm by the 1,10-phenanthroline method with a Hach DR 2800 portable spectrophotometer. PMS concentration was measured by a modified iodide spectrophotometry method [42]. The pH was measured using a Leici pH meter (Shanghai, China). The intermediate products of atrazine were detected by liquid chromatography-mass spectrometry-mass spectrometry (LC/MS/MS, Agilent 1290 series LC, 6460 Triple Quad LC/MS), and the details can be found in Text S2.

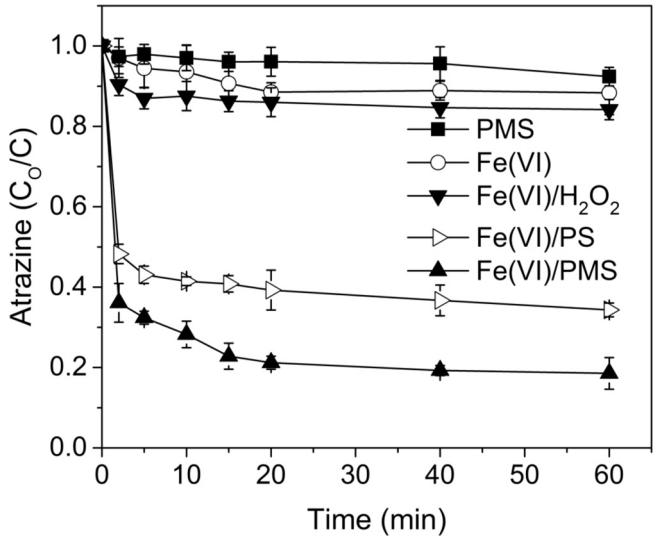

Fig. 1. Degradation kinetics of atrazine under various oxidants. Conditions: [H_2O_2] = [PS] = [PMS] = 5.0 mM, [Fe(VI)] = 2.5 mM, [atrazine] = 46.5 μM, pH 6.0, 25 °C.

3. Results and discussion

3.1. Catalytic degradation of atrazine

The degradation of atrazine was investigated using various oxidation processes, including the Fe(VI), PMS, Fe(VI)/H_2O_2, Fe(VI)/PS, and Fe(VI)/PMS processes. As shown in Fig. 1, PMS alone was ineffective at degrading atrazine, demonstrating that PMS alone could not generate reactive radicals, which was consistent with the study of Guan et al. [43]. In the presence of Fe(VI), 11.7% degradation was obtained within 60 min. As reported by Zajíček et al. [34], the almost complete degradation of atrazine was achieved by Fe(VI) at pH 6.0 and a molar ratio of 75. In the Fe(VI)/H_2O_2 process, 15.9% of atrazine was degraded. It has been reported that the combination of Fe(VI) and H_2O_2 can effectively enhance the remediation efficiency of groundwater contaminated with organic pollutants [35]. When the Fe(VI)/PS or Fe (VI)/PMS processes were used, the degradation of atrazine was obviously enhanced, resulting in the efficiencies of 65.7% and 81.5%, respectively. Moreover, the combined use of Fe(VI) and PMS for atrazine degradation was much higher than the sum of Fe(VI) and PMS alone, suggesting a synergistic effect between Fe(VI) and PMS. Meanwhile, the pH values before and after reaction are shown in Fig. S1. In the Fe(VI)/H_2O_2 process, pH increased from 6.10 to 10.77 after reaction. This could be explained by the reaction of H_2O_2 with Fe(VI) as proposed by Rush et al. [44], leading to increased pH (Eq. (3)). Conversely, pH values in the Fe(VI)/PS and Fe(VI)/PMS processes decreased. In particular, the pH of Fe(VI)/PMS sharply dropped from 6.09 to 3.17, which was attributed to the strong acidity of PMS. To evaluate the contribution of the acidic effect induced by PMS addition, we conducted the degradation of atrazine by Fe(VI) alone at an initial pH of 3.0 (Fig. S2). The degradation efficiency of atrazine (31.2%) at pH 3.0 by Fe(VI) was higher than that at pH 6.0, but still less than that of Fe (VI)/PMS. These results indicated that the superiority of Fe(VI)/PMS was not mainly attributed to the acidity effect of PMS, but to other factors as well, such as the involvement of reactive species. A synergistic effect was also observed in the degradation of fluoroquinolones by the Fe(VI)/PMS process [39]. Additionally, the Fe(VI)/PMS process degrades atrazine more efficiently than do other PMS activation methods (Table S1).

$$2FeO_4^{2-} + 3H_2O_2 + 2H_2O \rightarrow 2Fe(OH)_3 + 3O_2\uparrow + 4OH^- \quad (3)$$

3.2. Effects of PMS and Fe(VI) doses

The effects of the PMS and Fe(VI) doses on atrazine degradation are shown in Fig. 2. The degradation of atrazine by Fe(VI)/PMS followed a two-stage reaction (Fig. 2a). The degradation efficiency was sharply increased at the initial stage (t < 2.0 min) and then slowed down. Similar phenomenon occurred in the degradation of sulfamonomethoxine by Fe_3O_4/PS system [45]. As the Fe(VI) dose increased from 0.5 mM to 6.0 mM, the degradation efficiency was significantly increased. Specifically, in the presence of 6.0 mM, complete degradation was achieved within 20 min. There might be two reasons for the rapid and efficient degradation of atrazine. On one hand, Fe(VI) itself could oxidize atrazine by attacking alkyl-chain moieties, as demonstrated by LC/MS/MS analysis (Fig. S3). On the other hand, iron oxides/hydroxides or Fe(III) ion, generated from the reduction of Fe(VI) [29], might activate PMS to accelerate the degradation of atrazine. Additionally, the influence of PMS concentration on atrazine degradation was evaluated (Fig. 2b). The degradation efficiency of atrazine was enhanced from 51.8% to 80.3% with an increase in the initial PMS concentration from 1.2 to 5.0 mM. However, when PMS concentration further increased to 7.5 mM, its degradation efficiency dropped to 74.8% after 60 min. This was attributed to the production of more $SO_4^{\cdot -}$ with an increase in PMS concentration, but excess $SO_4^{\cdot -}$ could be consumed by itself and excess PMS (Eqs. (4) and (5)), leading to the decreased degradation.

$$SO_4^{\cdot -} + SO_4^{\cdot -} \rightarrow S_2O_8^{2-} (\ k = 4.0 \times 10^8\ M^{-1}S^{-1}) \quad (4)$$

$$HSO_5^- + SO_4^{\cdot -} \rightarrow SO_5^{\cdot -} + HSO_4^- (\ k < 10^5\ M^{-1}S^{-1}) \quad (5)$$

3.3. Effect of pH

Fig. 2c shows the effect of solution pH on atrazine degradation during the Fe(VI)/PMS process. After 60 min reaction, degradation efficiencies of 64.3%, 73.8%, 81.7%, 80.7%, and 78.7% could be obtained at pH 3.0, 5.0, 6.0, 7.0, and 9.0, respectively. This result is consistent with a previous study that the optimal pH for atrazine degradation by the Co(II)/PMS process is neutral [25]. The pK_a of atrazine is 1.7 [46], and thereby, the charge of atrazine remained unchanged within the pH range investigated in this study. In fact, pH can affect the fractions of PMS species. The pK_{a1} and pK_{a2} of PMS are 0 and 9.4, respectively, so HSO_5^- is the dominant species in the pH range of 3.0–9.0 [47]. In addition, Fe(VI) exists in four different protonated forms (Eqs. (6)–(8)) [48], among which $HFeO_4^-$ is the major species at pH 3.5–7.3, and its reactivity is higher than that of FeO_4^{2-}. Fe(VI) is the most stable form at pH 9.0; thus, it was difficult to activate PMS to generate reactive species. However, in acidic-neutral conditions, the self-decay of Fe(VI) could induce the formation of maghemite/lepidocrocite (γ-Fe_2O_3/γ-FeOOH) particles [29]. The pH_{PZC} (pH at the point of zero charge) of Fe(VI) resultant particles was 6.9 (Fig. S4), leading to a positive charge at pH < pH_{PZC} and negative charge at pH > pH_{PZC}. In acidic conditions, excess H^+ could react with HSO_5^- to form hydrogen bonds, which hindered the interaction between HSO_5^- and the positively charged of Fe(VI) resultant particles, reducing atrazine degradation. Overall, the Fe(VI)/PMS process is feasible for the degradation of atrazine from actual water, because actual water has a pH range of 5.0–9.0.

$$H_3FeO_4^+ \rightarrow H^+ + H_2FeO_4 (pKa = 1.6) \quad (6)$$

$$H_2FeO_4 \rightarrow H^+ + HFeO_4^- (pKa = 3.5) \quad (7)$$

$$HFeO_4^- \rightarrow H^+ + FeO_4^{2-} (pKa = 7.3) \quad (8)$$

3.4. Effect of temperature

The influence of temperature on atrazine degradation was evaluated in the range of 15–40 °C (Fig. 2d). As observed, the degradation

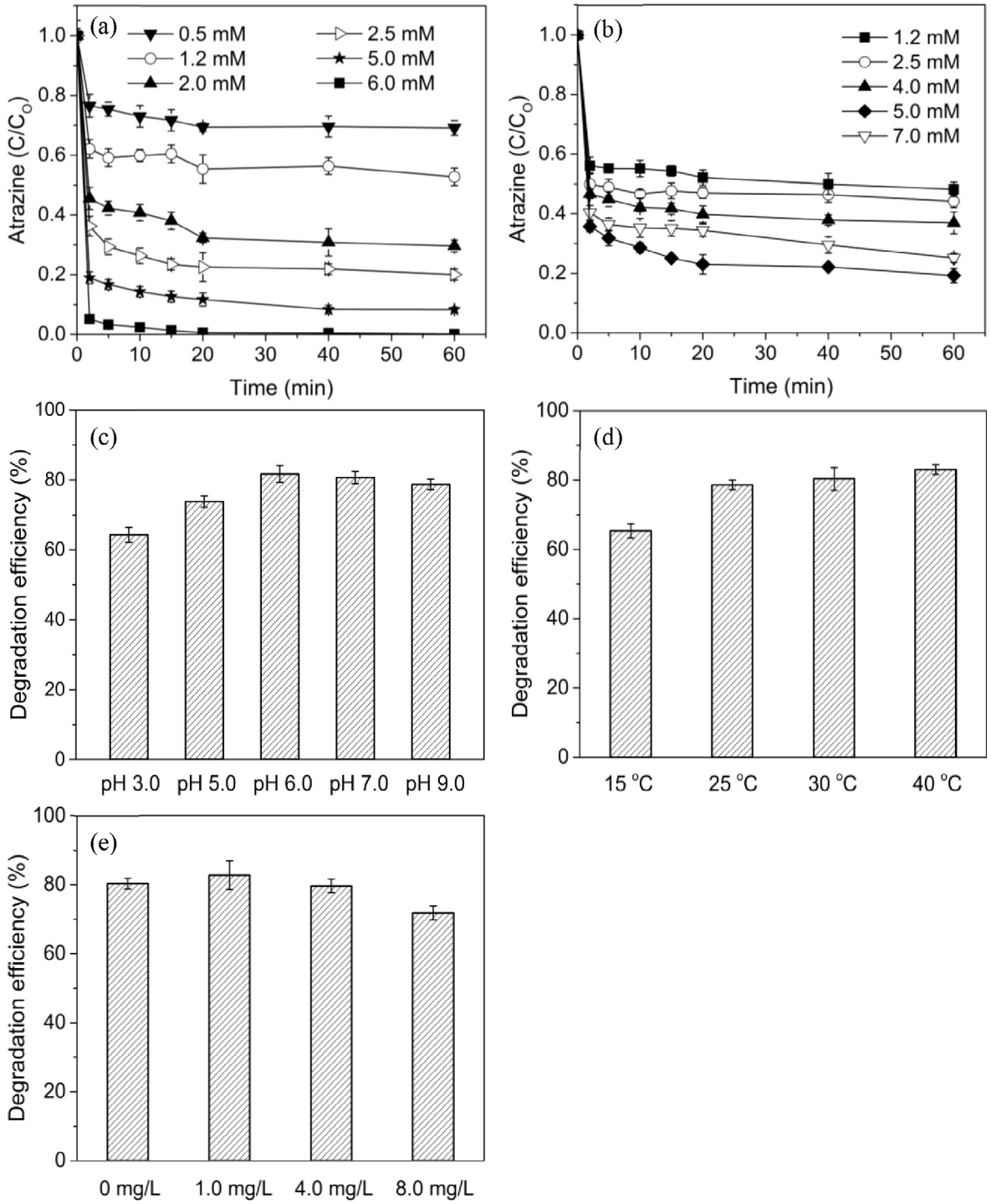

Fig. 2. Degradation kinetics of atrazine at various conditions. (a) Effect of Fe(VI) dose; (b) PMS concentration; (c) initial pH; (d) temperature; and (e) NOM on atrazine degradation by Fe(VI)/PMS process. Conditions: [atrazine] = 46.5 μM, [PMS] = 5.0 mM (for a, c, d and e), [Fe(VI)] = 2.5 mM (for b, c, d and e), pH 6.0 (for a, b, d and e), 25 °C (for a, b, c and e), after 60 min reaction (for c, d and e).

efficiency of atrazine was increased with increasing temperature. Remarkably, after 60 min reaction, 63.4% of atrazine was degraded at 15 °C, and 78.7% degradation was observed when the temperature was raised to 25 °C. This result suggested that high temperature might promote the reduction of Fe(VI) and the fast decomposition of PMS, thus generating more reactive species responsible for atrazine degradation.

3.5. Effect of NOM

Humic acid is the major constituent of NOM, and its major functional groups include carboxylic, phenolic, alcoholic hydroxyl, ketone and quinone groups. In this study, humic acid was used to evaluate the effect of NOM on atrazine degradation (Fig. 2e). The content of humic acid is expressed in terms of the TOC value (mg/L). The addition of humic acid (below 4.0 mg/L) is favorable for atrazine degradation. This may be attributed to the oxygen-containing functional groups of humic acid, which can activate PMS to generate free radicals. Previous studies

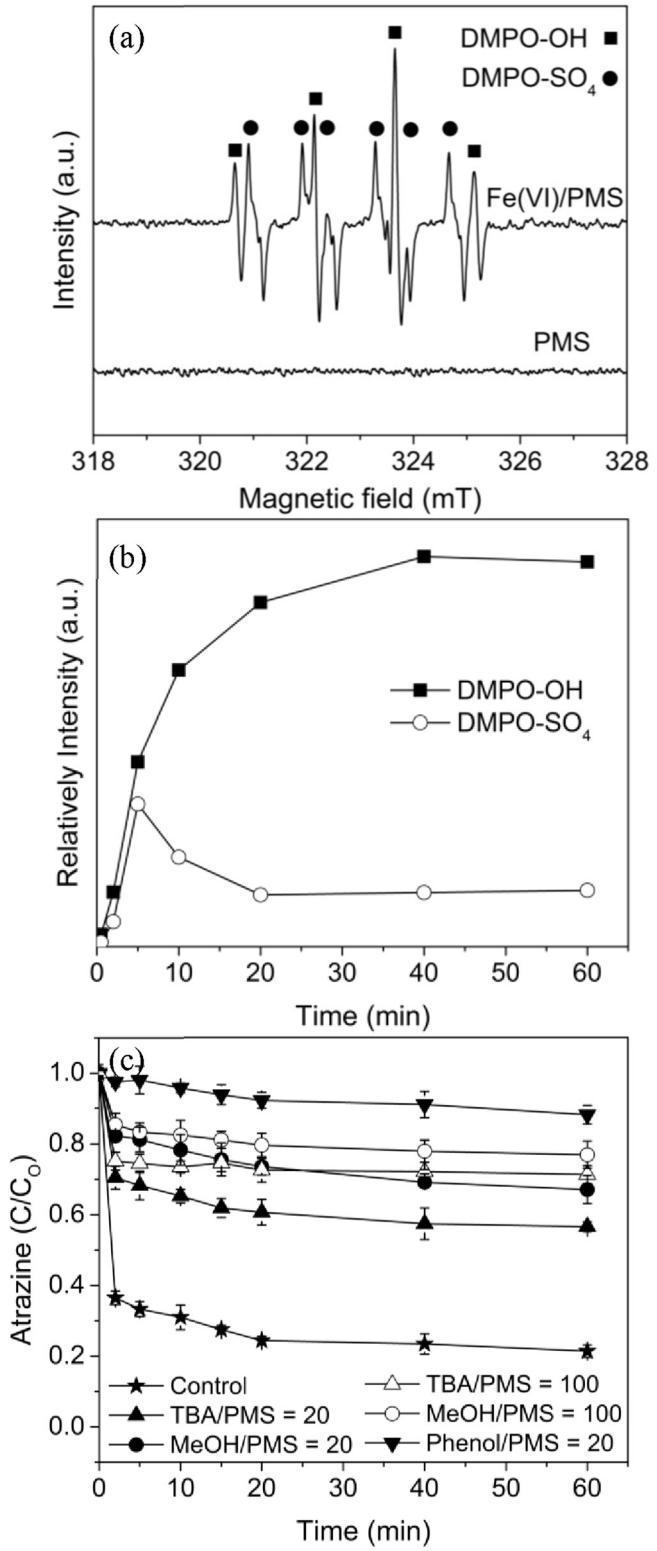

Fig. 3. (a) ESR spectra in the PMS and Fe(VI)/PMS processes at 5.0 min. (b) The intensity variations of DMPO-OH and DMPO-SO_4 during Fe(VI)/PMS process. (c) Effect of radical scavengers on atrazine degradation. Conditions: [PMS] = 5.0 mM, [Fe(VI)] = 2.5 mM, [atrazine] = 46.5 μM, [DMPO] = 100 mM, pH 6.0, 25 °C.

have reported that semiquinone radicals generated from humic acid, quinones, and phenols can efficiently stimulate PS to produce $SO_4^{\cdot -}$ [49,50]. Moreover, $SO_4^{\cdot -}$ is less influenced by NOM than ·OH, since $SO_4^{\cdot -}$ preferably reacts with organic pollutants via an electron transfer mechanism [51,52]. Jiang et al. [53] found that UV_{254} decreased by 21–74% for 10 mg/L humic acid at pH 7.8, with the addition of 0.04–0.82 mM of Fe(VI) [53]. In this study, the content of Fe(VI) was 2.5 mM, which was enough to alleviate the inhibition of atrazine degradation by NOM. However, with an increase in humic acid to 8.0 mg/L, the degradation efficiency decreased to 71.7%.

3.6. Radical identification and degradation mechanisms

To explore the generation and evolution of the reactive species during the Fe(VI)/PMS process, ESR studies were employed using DMPO as a spin-trapping agent (Fig. 3a). In the Fe(VI)/PMS process, the signals of DMPO-SO_4 (aN = 13.7 G, aH = 10.0 G, aH = 1.41 G, and aH = 0.78 G) and DMPO-OH (aH = 15.0 G and aN = 14.9 G) were both identified based on their hyperfine splitting constants, which was well consistent with a previous study [54]. Meanwhile, the highest peak intensities of DMPO-SO_4 were observed at 5.0 min, and then the intensities decreased and became stable after 20 min (Fig. 3b), which indicated a substantial consumption of $SO_4^{\cdot -}$ for atrazine degradation. However, the peak intensities of DMPO-OH increased rapidly within first 20 min and remained almost stable afterwards. This result indicated that $SO_4^{\cdot -}$ might be the dominant radicals. To further examine the relative contributions of ·OH and $SO_4^{\cdot -}$ to atrazine degradation, quenching experiments were conducted (Fig. 3c). It is generally accepted that MeOH is used to effectively scavenge both $SO_4^{\cdot -}$ and ·OH, since its reaction rate constants with $SO_4^{\cdot -}$ and ·OH are respectively 0.9–1.3 × 10^7 M^{-1} s^{-1} and 8.0–10 × 10^8 M^{-1} s^{-1} [55], while TBA has 3 order of magnitude higher reactivity for ·OH than for $SO_4^{\cdot -}$ (k_{SO4-} = 4.0–9.1 × 10^5 M^{-1} s^{-1}, $k_{\cdot OH}$ = 3.8–7.6 × 10^8 M^{-1} s^{-1}) [28]. The degradation efficiency of atrazine significantly decreased from 78.6% to 43.4% at TBA/PMS molar ratio of 20. As the molar ratio of TBA/PMS increased to 100, the degradation efficiency sharply decreased to 28.7% within 2 min and then remained almost stable. Moreover, the inhibition effect of MeOH was stronger than that of TBA. Specifically, with an increase in the molar ratio of MeOH/PMS to 100, degradation efficiency was decreased to 23.1%. In addition, phenol was a more effective quenching agent for the total radicals due to its high reactivity with ·OH and $SO_4^{\cdot -}$ ($k_{SO4\cdot -}$ = 6.6 × 10^9 M^{-1} s^{-1}, $k_{\cdot OH}$ = 8.8 × 10^9 M^{-1} s^{-1}) [56]. Compared to MeOH or TBA, phenol showed stronger inhibition of atrazine degradation. This inhibition is attributed to the hydrophobic property of phenol, which makes it easier for phenol to approach the surface of the solid catalyst [57]. Moreover, nitrobenzene was selected as a ·OH probe compound because it is resistant to $SO_4^{\cdot -}$ [43]. Compared to atrazine degradation, the degradation of nitrobenzene by Fe(VI)/PMS could be ignored, as could the nitrobenzene degradation efficiency of 8.2% (Fig. S5). Hence, it can be concluded that $SO_4^{\cdot -}$ is the predominant reactive species responsible for atrazine degradation.

To obtain insights into the active sites of the Fe(VI) resultant particles, Fe(VI) particles before and after reaction were analyzed by XRD and XPS techniques. The XRD results (Fig. 4a) showed that the main characteristic peaks of Fe(VI) were consistent with an orthorhombic crystal system with space group D_{2h} (Pnma) [58]. After reaction, most of the characteristic peaks disappeared, which indicated that Fe(VI) was amorphous. Instead, some new peaks (30.1°, 35.5°, 57.2°, and 62.3°) were presented at the positions of the most intensive diffraction lines of γ-Fe_2O_3 [59]. The self-decomposition of Fe(VI) could form iron oxide particles with a core/shell (γ-Fe_2O_3/γ-FeOOH) structure, as observed by in-field ^{57}Fe Mössbauer spectroscopy [29]. Prucek et al. [60] also found a similar result in the removal of arsenite and arsenate by Fe(VI). This could be further characterized by XPS. After reaction, a strong peak observed at 711.8 eV was attributed to γ-Fe_2O_3 (Fig. 4(b)). These results confirmed that the Fe(VI) resultant particle contained γ-Fe_2O_3.

In addition, Sharma [61] proposed that the reactions of Fe(VI) with organic pollutants involve one-electron or two-electron transfer mechanisms with the formation of perferryl (V) and ferryl (IV);

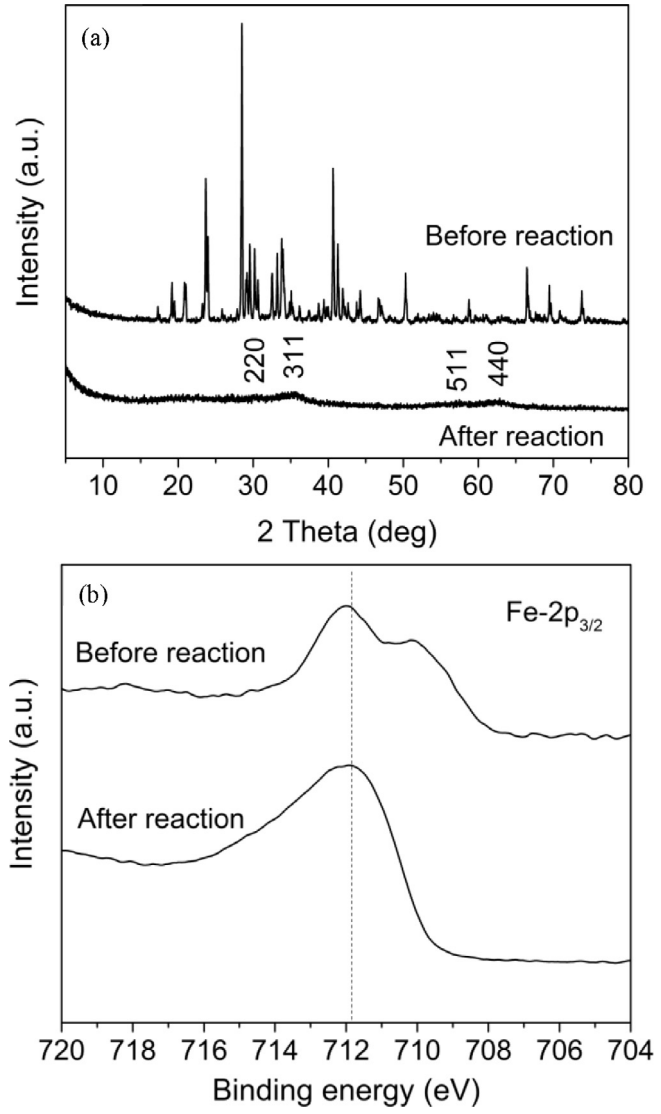

Fig. 4. (a) XRD pattern and (b) XPS high-resolution Fe $2p_{3/2}$ spectra of Fe(VI) resultant particles before and after reaction.

consequently, Fe(II) and Fe(III) are the final iron products, respectively. For this purpose, we monitored the changes in concentrations of Fe(II) and Fe(III) in solution (Fig. 5). The concentration of Fe(III) increased rapidly to 4.50 mg/L within 5 min and decreased to 0.51 mg/L after 15 min. Fe(III) could be obtained by the reduction of Fe(VI), while the content of Fe(III) was very low, because adding 49.5 mg Fe(VI) to 100 mL initial solution was equivalent to 140 mg/L Fe(III). The variation of Fe(II) was similar and its maximum concentration reached 1.61 mg/L in the first 2 min, which corresponded well to the rapid degradation of atrazine. In our previous study, Fe(II) ion was involved in the generation of ·OH and $SO_4^{\cdot -}$ for atrazine degradation [24]. After 20 min, the concentrations of Fe(III) and Fe(II) remained stable, which was well consistent with the decomposition of PMS (Fig. S6) and the relative intensity variations of DMPO-SO_4. This stability might be due to the coagulation of Fe(III), thus decreasing the concentration of iron ions and the decomposition of PMS. Cheng et al. [10] observed that Fe(II)/PMS could efficiently degrade atrazine due to the presence of both ·OH and $SO_4^{\cdot -}$, while coagulation did not. The formed γ-Fe_2O_3 particles could be further used to activate PMS. Both ·OH and $SO_4^{\cdot -}$ have been identified as dominant reactive species in the Fe_2O_3/PMS process [41,62]. Furthermore, we used the leaching solution within 5 min and residual solid particles (γ-Fe_2O_3) to activate PMS (Fig. S7).

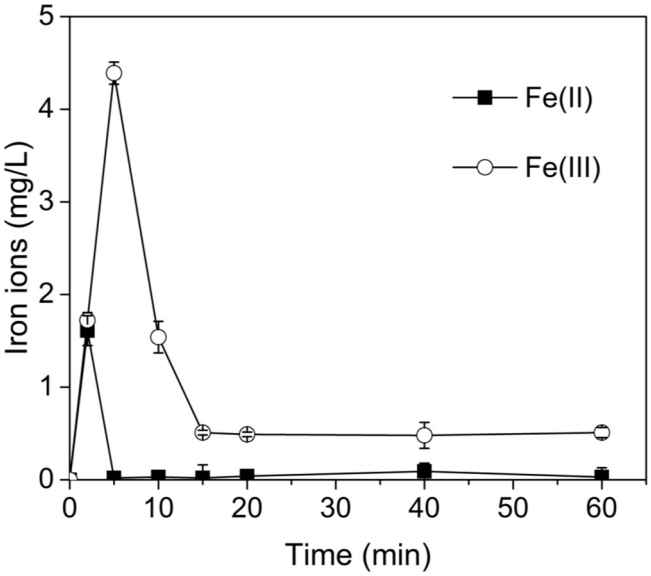

Fig. 5. Concentration of dissolved iron ions as a function of time. Conditions: [PMS] = 5.0 mM, [Fe(VI)] = 2.5 mM, [atrazine] = 46.5 μM, pH 6.0, 25 °C.

The result showed that γ-Fe_2O_3 particles are more effective in activating PMS, which corresponded to the atrazine degradation of 58.6%, indicating that the formation of ·OH and $SO_4^{\cdot -}$ could occur at the surface of Fe(VI) resultant particles.

On the basis of the above results, the mechanism of PMS activation by Fe(VI) is proposed and illustrated in Scheme 1. On one hand, PMS provided an acidic environment, where Fe(VI) was rapidly reduced to Fe(III) in solution (Eq. (1)). Fe(III) could react with PMS to produce Fe (II), according to Eq. (9). Subsequently, Fe(II) could activate PMS to produce $SO_4^{\cdot -}$ (Eq. (10)) [10]. On the other hand, the self-decomposition of Fe(VI) and the coagulation of Fe(III) ion led to the formation of γ-Fe_2O_3 particles. $SO_4^{\cdot -}$ could be produced by the exposed active sites of γ-Fe_2O_3 for PMS activation according to Eqs. (11)–(14). This activation mechanism was proposed by Ji et al. [41] for the Fe_2O_3/PMS process. Finally, $SO_4^{\cdot -}$ could react with H_2O to generate ·OH (Eq. (15)).

$$Fe^{3+} + HSO_5^- \rightarrow Fe^{2+} + SO_5^{\cdot -} + H^+ \quad (9)$$

$$Fe^{2+} + HSO_5^- \rightarrow Fe^{3+} + SO_4^{\cdot -} + OH^- \quad (10)$$

$$\equiv Fe^{3+}{-}OH + HSO_5^- \rightarrow \equiv Fe^{3+}{-}SO_5^- + H_2O \quad (11)$$

$$\equiv Fe^{3+}{-}SO_5^- + H_2O \rightarrow \equiv Fe^{2+}{-}OH + SO_5^{\cdot -} + H^+ \quad (12)$$

$$\equiv Fe^{2+}{-}OH + HSO_5^- \rightarrow \equiv Fe^{2+}{-}SO_5^- + H_2O \quad (13)$$

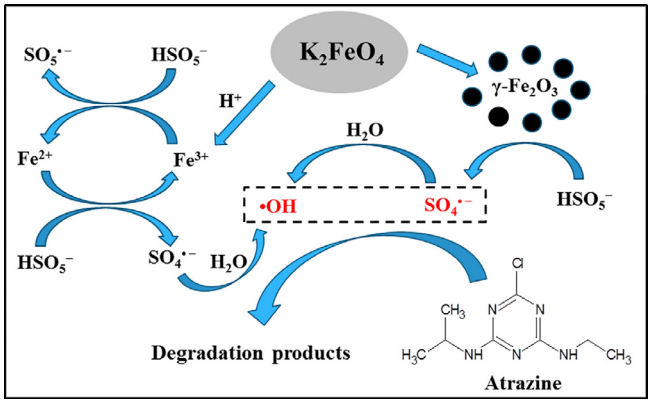

Scheme 1. Degradation mechanisms of atrazine by Fe(VI)/PMS process.

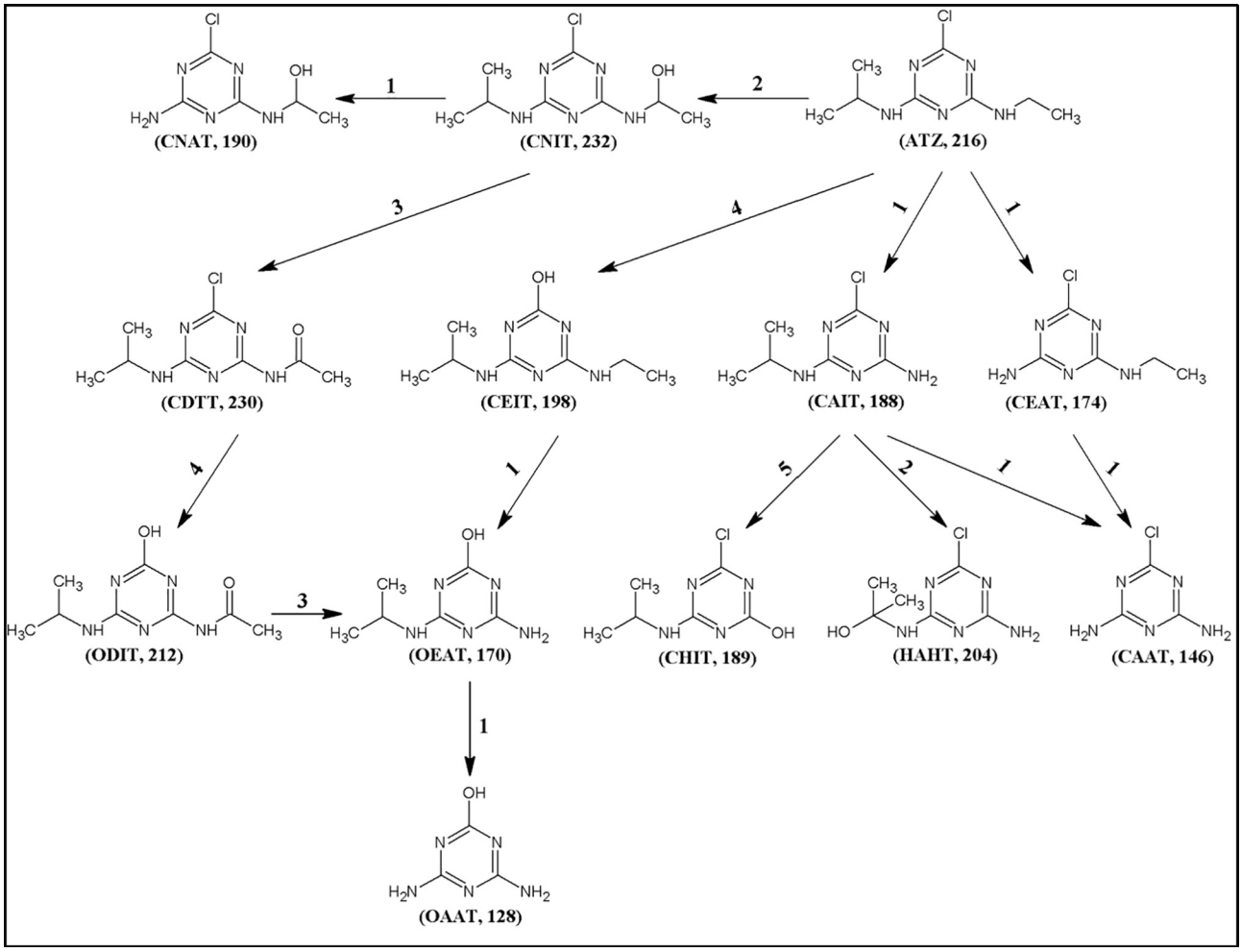

Scheme 2. The proposed degradation pathways of atrazine in the Fe(VI)/PMS process. (1) dealkylation, (2) alkylic hydroxylation, (3) alkylic oxidation, (4) dechlorination- hydroxylation, and (5) deamination-hydroxylation.

$$\equiv Fe^{2+}{-}SO_5^- + H_2O \rightarrow \equiv Fe^{3+}{-}OH + SO_4^{\cdot -} + OH^- \quad (14)$$

$$SO_4^{\cdot -} + H_2O \rightarrow SO_4^{2-} + \cdot OH + H^+ \quad (15)$$

3.7. Pathways for atrazine degradation

To elucidate the pathways of atrazine degradation by Fe(VI)/PMS, its reaction intermediates were first identified by LC/MS/MS technique. The retention time, molecular weight, name, abbreviation and structure of the products are summarized in Table S2. Fig. S8 depicts the total ion chromatogram for atrazine degradation in 60 min. In addition to atrazine, fourteen possible products were detected. Based on the degradation products identified, possible degradation pathways for atrazine were proposed and are presented in Scheme 2. Initially, $SO_4^{\cdot -}/\cdot OH$ were produced in the Fe(VI)/PMS process; subsequently, they attacked the alkyl side chains of atrazine to form CAIT and CEAT and were further dealkylated to CAAT. As reported by Ji et al. [25], $SO_4^{\cdot -}/\cdot OH$ preferably reacts with atrazine via attacking the carbon adjacent to nitrogen by H-abstraction, resulting in the formation of a carbon-centered radical. The reaction of the carbon-centered radical with oxygen yields a peroxide radical, which is converted to atrazine-imine by the loss of per-hydroxyl radical and is further hydrolyzed to CAIT and CEAT. Lutze et al. [51] indicated that 63.0% of atrazine was degraded based on $SO_4^{\cdot -}$ via dealkylation (CAIT + CEAT) and the molar ratio of CAIT to CEAT was almost 10. HAHT and CHIT could be formed from CAIT via alkylic hydroxylation and deamination-hydroxylation, respectively. This finding is well consistent with the results proposed by Khan et al. [19], who investigated the kinetics and mechanism of atrazine degradation under UV irradiation with H_2O_2, PS and PMS. In addition, the carbon-centered radical mentioned above could be attacked by ·OH to form CNIT. Nevertheless, CNIT is unstable and forms a carbon radical compound by $SO_4^{\cdot -}/\cdot OH$ from H-abstraction. This radical compound can react with oxygen and yield a peroxy radical intermediate which is eventually transformed to CDTT. CDTT might be also produced by the oxidation of carbinolamine intermediate by $SO_4^{\cdot -}/\cdot OH$ [63], as described in Eq. (16). Besides, CNIT could undergo dealkylation to give rise to CNAT. Chen et al. [64] found that the cleavage of the C-Cl bond in atrazine molecules was the easiest due to its longest bond length (1.734 Å) and relatively low bond polarity (0.293). Ji et al. [25] proposed that the dechlorination-hydroxylation of atrazine could be triggered by HO-adduct radical. As a result, ODIT and CEIT could be generated via dechlorination-hydroxylation. Subsequently, ODIT and CEIT undergo alkylic oxidation and dealkylation, respectively, to yield OEAT, which is eventually transformed to OAAT. In brief, atrazine can be oxidized through dechlorination-hydroxylation, dealkylation, deamination-hydroxylation, alkylic hydroxylation, and alkylic oxidation, among which dealkylation and alkylic oxidation are the predominant degradation pathways.

$$RNHCHOHCH_3 + SO_4^{\cdot -}/\cdot OH \rightarrow RNHCHOHCH_3(\text{acetamide}) \quad (16)$$

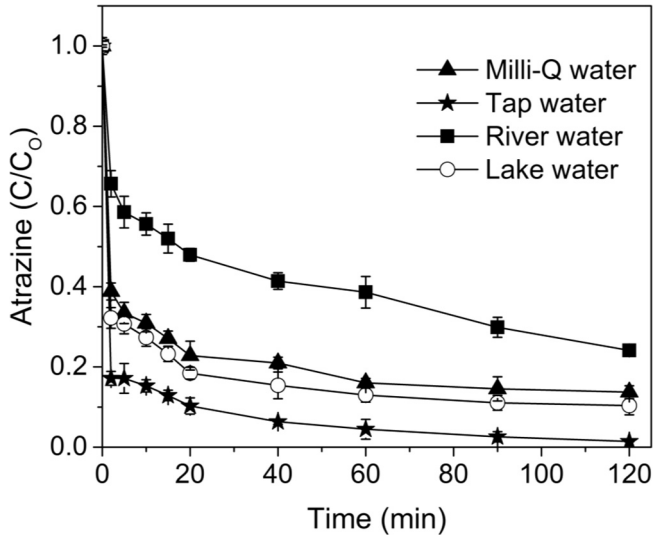

Fig. 6. Degradation of atrazine by Fe(VI)/PMS in various types of water. Conditions: [PMS] = 5.0 mM, [Fe(VI)] = 2.5 mM, [atrazine] = 46.5 μM, 25 °C.

3.8. Environmental applications

Considering the practical application of the Fe(VI)/PMS process, different kinds of natural waters were used as water background matrices in this study. The properties of the water samples are shown in Table S3. Fig. 6 presents the degradation of atrazine from various water samples in the Fe(VI)/PMS process. The degradation of atrazine was found to be the most efficient in tap water, and complete degradation was achieved in 120 min. In river water, the degradation efficiency was still higher than that in Milli-Q water, but lower than that in tap water, which was ascribed to the relatively high pH and TOC (Table S2). Guan et al. [43] conducted the degradation of atrazine by $CuFe_2O_4$/PMS in actual waters, suggesting that it might be affected by pH, TOC, and alkalinity. Nevertheless, since lake water contained a higher pH and TOC (almost twice as much as river water), the degradation was inhibited. In lake water, the degradation efficiency was 61.4% within 60 min, and further increased to 75.9% with a prolonged reaction time of 120 min. This result indicated that the degradation efficiency of atrazine by the Fe(VI)/PMS process was dependent on the water matrix.

4. Conclusions

This study comprehensively explored the degradation of atrazine by the Fe(VI)/PMS process. The following conclusions were drawn:

1. Fe(VI)/PMS can efficiently degrade atrazine in aqueous solutions, and complete degradation is obtained within 20 min at initial concentrations of 6.0 mM Fe(VI), 5.0 mM PMS, 25 °C, and pH 6.0.
2. The degradation of atrazine is enhanced with an increase in Fe(VI) dose (0.5–6.0 mM), PMS concentration (1.2–5.0 mM), or temperature (15–40 °C). NOM concentration less than 4.0 mg/L is favorable for atrazine degradation.
3. Both $SO_4^{\cdot -}$ and ·OH are generated in the Fe(VI)/PMS process, while $SO_4^{\cdot -}$ is the dominant reactive species responsible for atrazine degradation.
4. *In situ*-generated γ-Fe_2O_3 particles from Fe(VI) reduction could activate PMS.
5. On the basis of the LC/MS/MS technique, the pathways for atrazine degradation using Fe(VI)/PMS were proposed.
6. The degradation of atrazine by Fe(VI)/PMS remained highly efficient in real waters and was suitable for the wide range pH values in actual water.

Acknowledgements

This work was supported by the project of National Natural Science Foundation of China (Grant No.: 51478172, 51278464, and 51521006), the Natural Science Foundation of Zhejiang Province of China (Grant No.: LY17E080002) and the Department of Science and Technology of Hunan Province of China (Contract No.: 2017JJ2029 and 2017SK2362).

Appendix A. Supplementary data

Supplementary data associated with this article can be found, in the online version, at https://doi.org/10.1016/j.cej.2018.06.133.

References

[1] N. Graziano, M.J. Mcguire, A. Roberson, C. Adams, H. Jiang, N. Blute, National atrazine occurrence monitoring program using the Abraxis ELISA method, Environ. Sci. Technol. 40 (2006) (2004) 1163–1171.
[2] Y. Cheng, H.J. He, C.P. Yang, G.M. Zeng, X. Li, H. Chen, G.L. Yu, Challenges and solutions for biofiltration of hydrophobic volatile organic compounds, Biotechnol. Adv. 34 (2016) 1091–1102.
[3] R.I. Bonansea, M.V. Amé, D.A. Wunderlin, Determination of priority pesticides in water samples combining SPE and SPME coupled to GC-MS. A case study: suquía River basin (Argentina), Chemosphere 90 (2013) 1860–1869.
[4] European Commission, SANCO/10232/2006, Quality Control Procedures For Pesticide Residues Analysis, European Union, Brussels, 2006.
[5] T.B. Hayes, V. Khoury, A. Narayan, M. Nazir, A. Park, T. Brown, L. Adame, E. Chan, D. Buchholz, T. Stueve, S. Gallipeau, Atrazine induces complete feminization and chemical castration in male African clawed frogs (*Xenopus laevis*), Proc. Natl. Acad. Sci. U.S.A. 107 (2010) 4612–4617.
[6] A.N. Edginton, C. Rouleau, Toxicokinetics of 14C-atrazine and its metabolites in stage-66 *Xenopus laevis*, Environ. Sci. Technol. 39 (2005) 8083–8089.
[7] A.L. Ahmad, L.S. Tan, S.R.A. Shukor, Dimethoate and atrazine retention from aqueous solution by nanofiltration membranes, J. Hazard. Mater. 151 (2008) 71–77.
[8] S.H. Wu, H.J. He, X. Inthapanya, C.P. Yang, L. Lu, G.M. Zeng, Z.F. Han, Role of biochar on composting of organic wastes and remediation of contaminated soils-a review, Environ. Sci. Pollut. Res. 24 (2017) 16560–16577.
[9] C.Y. Zhu, W.L. Yang, H.J. He, C.P. Yang, J.P. Yu, X. Wu, G.M. Zeng, S. Tarre, M. Green, Preparation, performances and mechanisms of magnetic *Saccharomyces cerevisiae*, bionanocomposites for atrazine removal, Chemosphere 200 (2018) 380–387.
[10] X.X. Cheng, H. Liang, D.A. Ding, X.B. Tang, B. Liu, X.W. Zhu, Z.D. Gan, D.J. Wu, G.B. Li, Ferrous iron/peroxymonosulfate oxidation as a pretreatment for ceramic ultrafiltration membrane: control of natural organic matter fouling and degradation of atrazine, Water Res. 113 (2017) 32–41.
[11] J.P. Yu, H.J. He, W.L. Yang, C.P. Yang, G.M. Zeng, X. Wu, Magnetic bionanoparticles of *Penicillium* sp. yz11-22N2 doped with Fe_3O_4 and encapsulated within PVA-SA gel beads for atrazine removal, Bioresour. Technol. 260 (2018) 196–203.
[12] Z. Yan, H.J. He, C.P. Yang, G.M. Zeng, L. Luo, P.P. Jiao, H.R. Li, L. Lu, Biodegradation of 3,5-dimethyl-2,4-dichlorophenol in saline wastewater by newly isolated *Penicillium* sp. yz11-22N2, J. Environ. Sci. 57 (2017) 211–220.
[13] H.J. He, Y.J. Chen, X. Li, Y. Cheng, C.P. Yang, G.M. Zeng, Influence of salinity on microorganisms in activated sludge processes: a review, Int Biodeter. Biodegr. 119 (2017) 520–527.
[14] P. Neta, V. Madhavan, H. Zemel, R.W. Fessenden, Rate constants and mechanism of reaction of sulfate radical anion with aromatic compounds, J. Am. Chem. Soc. 99 (1977) 163–164.
[15] R.X. Li, C.P. Yang, H. Chen, G.M. Zeng, G.L. Yu, J.Y. Guo, Removal of triazophos pesticide from wastewater with Fenton reagent, J. Hazard. Mater. 167 (2009) 1028–1032.
[16] L.J. Xu, J.L. Wang, Magnetic nanoscaled Fe_3O_4/CeO_2 composite as an efficient Fenton-like heterogeneous catalyst for degradation of 4-chlorophenol, Environ. Sci. Technol. 46 (2012) 10145–10151.
[17] W.D. Oh, Z.L. Dong, T.T. Lim, Generation of sulfate radical through heterogeneous catalysis for organic contaminants removal: current development, challenges and prospects, Appl. Catal. B: Environ. 194 (2016) 169–201.
[18] Y. Lin, S.H. Wu, X. Li, X. Wu, C.P. Yang, G.M. Zeng, Y.R. Peng, Q. Zhou, L. Lu, Microstructure and performance of Z-scheme photocatalyst of silver phosphate modified by MWCNTs and Cr-doped $SrTiO_3$ for malachite green degradation, Appl. Catal. B: Environ. 227 (2018) 557–570.
[19] J.A. Khan, X.X. He, N.S. Shah, H.M. Khan, E. Hapeshi, D. Fatta-Kassinos, D.D. Dionysiou, Kinetic and mechanism investigation on the photochemical degradation of atrazine with activated H_2O_2, $S_2O_8^{2-}$ and HSO_5^-, Chem. Eng. J. 252 (2014) 393–403.
[20] Y.F. Ji, C.X. Dong, D.Y. Kong, J.H. Lu, Q.S. Zhou, Heat-activated persulfate oxidation of atrazine: Implications for remediation of groundwater contaminated by herbicides, Chem. Eng. J. 263 (2015) 45–54.
[21] Y.C. Lee, S.L. Lo, P.T. Chiueh, D.G. Chang, Efficient decomposition of perfluorocarboxylic acids in aqueous solution using microwave-induced persulfate,

Water Res. 43 (2009) 2811–2816.
[22] L.B. Peng, L. Wang, X.T. Hu, P.H. Wu, X.Q. Wang, C.M. Huang, X.Y. Wang, D.Y. Deng, Ultrasound assisted, thermally activated persulfate oxidation of coal tar DNAPLs, J. Hazard. Mater. 318 (2016) 497–506.
[23] O.S. Furman, A.L. Teel, R.J. Watts, Mechanism of base activation of persulfate, Environ. Sci. Technol. 44 (2010) 6423–6428.
[24] S.H. Wu, H.J. He, X. Li, C.P. Yang, G.M. Zeng, B. Wu, S.Y. He, L. Lu, Insights into atrazine degradation by persulfate activation using composite of nanoscale zero-valent iron and graphene: performances and mechanisms, Chem. Eng. J. 341 (2018) 126–136.
[25] Y.F. Ji, C.X. Dong, D.Y. Kong, J.H. Lu, New insights into atrazine degradation by cobalt catalyzed peroxymonosulfate oxidation: kinetics, reaction products and transformation mechanisms, J. Hazard. Mater. 285 (2015) 491–500.
[26] M.G. Antoniou, A.A.D.L. Cruz, D.D. Dionysiou, Degradation of microcystin-LR using sulfate radicals generated through photolysis, thermolysis and e^- transfer mechanisms, Appl. Catal. B: Environ. 96 (2010) 290–298.
[27] A.G. Miroshnichenko, V.A. Lunenok-Burmakina, A quantum-mechanical study of the structure of inorganic derivatives of hydrogen peroxide, Theor. Exp. Chem 11 (1976) 320–325.
[28] G.P. Anipsitakis, D.D. Dionysiou, Radical generation by the interaction of transition metals with common oxidants, Environ. Sci. Technol. 38 (2004) 3705–3712.
[29] R.P. Kralchevska, R. Prucek, J. Kolařík, J. Tuček, L. Machala, J. Filip, V.K. Sharma, R. Zbořil, Remarkable efficiency of phosphate removal: ferrate(VI)-induced in situ sorption on core-shell nanoparticles, Water Res. 103 (2016) 83–91.
[30] S.H. Wu, Z.Q. Shen, C.P. Yang, Y.X. Zhou, X. Li, G.M. Zeng, S.J. Ai, H.J. He, Effects of C/N ratio and bulking agent on speciation of Zn and Cu and enzymatic activity during pig manure composting, Int Biodeter. Biodegr. 119 (2017) 429–436.
[31] V.K. Sharma, L. Chen, R. Zboril, Review on high valent Fe^{VI} (Ferrate): a sustainable green oxidant in organic chemistry and transformation of pharmaceuticals, ACS Sustain. Chem. Eng. 4 (2016) 18–34.
[32] Y.J. Jiang, J.E. Goodwill, J.E. Tobiason, D.A. Reckhow, Impacts of ferrate oxidation on natural organic matter and disinfection byproduct precursors, Water Res. 96 (2016) 114–125.
[33] Y. Lee, J. Yoon, U.V. Gunten, Kinetics of the oxidation of phenols and phenolic endocrine disruptors during water treatment with ferrate (Fe(VI)), Environ. Sci. Technol. 39 (2005) 8978–8984.
[34] P. Zajíček, M. Kolář, R. Prucek, V. Ranc, P. Bednář, R.S. Varma, V.K. Sharma, R. Zbořil, Oxidative degradation of triazine- and sulfonylurea-based herbicides using Fe(VI): The case study of atrazine and iodosulfuron with kinetics and degradation products, Sep. Purif. Technol. 156 (2015) 1041–1046.
[35] P. Lacina, S. Goold, Use of the ferrates (Fe(IV-VI)) in combination with hydrogen peroxide for rapid and effective remediation of water-laboratory and pilot study, Water. Sci. Technol. 72 (2015) 1869–1878.
[36] S.F. Sun, S.Y. Pang, J. Jiang, J. Ma, Z.S. Huang, J.M. Zhang, Y.L. Liu, C.B. Xu, Q.L. Liu, Y.X. Yuan, The combination of ferrate(VI) and sulfite as a novel advanced oxidation process for enhanced degradation of organic contaminants, Chem. Eng. J. 333 (2017) 11–19.
[37] J. Zhang, L. Zhu, Z.Y. Shi, Y. Gao, Rapid removal of organic pollutants by activation sulfite with ferrate, Chemosphere 186 (2017) 576–579.
[38] Q. Han, H.J. Wang, W.Y. Dong, T.Z. Liu, Y.L. Yin, Formation and inhibition of bromate during ferrate(VI)-Ozone oxidation process, Sep. Purif. Technol. 118 (2013) 653–658.
[39] M.B. Feng, L. Cizmas, Z.Y. Wang, V.K. Sharma, Synergistic effect of aqueous removal of fluoroquinolones by a combined use of peroxymonosulfate and ferrate(VI), Chemosphere 177 (2017) 144–148.
[40] J.E. Goodwill, Y.J. Jiang, D.A. Reckhow, J. Gikonyo, J.E. Tobiason, Characterization of particles from ferrate preoxidation, Environ. Sci. Technol. 49 (2015) 4955–4962.
[41] F. Ji, C.L. Li, X.Y. Wei, J. Yu, Efficient performance of porous Fe_2O_3 in heterogeneous activation of peroxymonosulfate for decolorization of Rhodamine B, Chem. Eng. J. 231 (2013) 434–440.
[42] C.J. Liang, C.F. Huang, N. Mohanty, R.M. Kurakalva, A rapid spectrophotometric determination of persulfate anion in ISCO, Chemosphere 73 (2008) 1540–1543.
[43] Y.H. Guan, J. Ma, Y.M. Ren, Y.L. Liu, J.Y. Xiao, L.Q. Lin, C. Zhang, Efficient degradation of atrazine by magnetic porous copper ferrite catalyzed peroxymonosulfate oxidation via the formation of hydroxyl and sulfate radicals, Water Res. 47 (2013) 5431–5438.
[44] J.D. Rush, Z.W. Zhao, B.H.J. Bielski, Reaction of ferrate (VI)/ferrate (V) with hydrogen peroxide and superoxide anion-a stopped-flow and premix pulse radiolysis study, Free. Radical. Res. 24 (1996) 187–198.
[45] J.C. Yan, M. Lei, L.H. Zhu, M.N. Anjum, J. Zou, H.Q. Tang, Degradation of sulfamonomethoxine with Fe_3O_4 magnetic nanoparticles as heterogeneous activator of persulfate, J. Hazard. Mater. 186 (2011) 1398–1404.
[46] S. Ahmed, M.G. Rasul, R. Brown, M.A. Hashib, Influence of parameters on the heterogeneous photocatalytic degradation of pesticides and phenolic contaminants in wastewater: a short review, J. Environ. Manage. 92 (2011) 311–330.
[47] M. Mahdi-ahmed, S. Chiron, Ciprofloxacin oxidation by UV-C activated peroxymonosulfate in wastewater, J. Hazard. Mater. 265 (2014) 41–46.
[48] V.K. Sharma, Potassium ferrate(VI): an environmentally friendly oxidant, Adv. Environ. Res. 6 (2002) 143–156.
[49] M. Ahmad, A.L. Teel, R.J. Watts, Mechanism of persulfate activation by phenols, Environ. Sci. Technol. 47 (2013) 5864–5871.
[50] G.D. Fang, J. Gao, D.D. Dionysiou, C. Liu, D.M. Zhou, Activation of persulfate by quinones: free radical reactions and implication for the degradation of PCBs, Environ. Sci. Technol. 47 (2013) 4605–4611.
[51] H.V. Lutze, S. Bircher, I. Rapp, N. Kerlin, R. Bakkour, M. Geisler, C.V. Sonntag, T.C. Schmidt, Degradation of chlorotriazine pesticides by sulfate radicals and the influence of organic matter, Environ. Sci. Technol. 49 (2015) 1673–1680.
[52] C.P. Yang, H.Y. Liu, S.L. Luo, X. Chen, H.J. He, Performance of modified electro-Fenton process for phenol degradation using bipolar graphite electrodes and activated carbon, J. Environ. Eng. ASCE 137 (2012) 613–619.
[53] J.Q. Jiang, S. Wang, Enhanced coagulation with potassium ferrate(VI) for removing humic substances, Environ. Eng. Sci. 20 (2003) 627–633.
[54] C.Q. Tan, N.Y. Gao, Y.J. Deng, S.Q. Zhou, J. Li, X.Y. Xin, Radical induced degradation of acetaminophen with Fe_3O_4 magnetic nanoparticles as heterogeneous activator of peroxymonosulfate, J. Hazard. Mater. 276 (2014) 452–460.
[55] H. Eibenberger, S. Steenken, P. O'Neill, D. Schulte-frohlinde, Pulse radiolysis and electron spin resonance studies concerning the reaction of $SO_4^{\cdot -}$ with alcohols and ethers in aqueous solution, J. Phys. Chem. 82 (1978) 749–750.
[56] H.Y. Liang, Y.Q. Zhang, S.B. Huang, I. Hussain, Oxidative degradation of *p*-chloroaniline by copper oxidate activated persulfate, Chem. Eng. J. 218 (2013) 384–391.
[57] J. Zhang, X.T. Shao, C. Shi, S.Y. Yang, Decolorization of Acid Orange 7 with peroxymonosulfate oxidation catalyzed by granular activated carbon, Chem. Eng. J. 232 (2013) 259–265.
[58] S. Licht, V. Naschitz, L. Halperin, N. Halperin, L. Lin, J. Chen, S. Ghosh, B. Liu, Analysis of ferrate(VI) compounds and super-iron Fe(VI) battery cathodes: FTIR, ICP, titrimetric, XRD, UV/VIS, and electrochemical characterization, J. Power Sources 101 (2001) 167–176.
[59] F.C.C. Oliveira, L.M. Rossi, R.F. Jardim, J.C. Rubim, Magnetic fluids based on γ-Fe_2O_3 and $CoFe_2O_4$ nanoparticles dispersed in ionic liquids, J. Phys. Chem. C. 113 (2009) 8566–8572.
[60] R. Prucek, J. Tuček, J. Kolařík, J. Filip, Z. Marušák, V.K. Sharma, R. Zbořil, Ferrate (VI)-induced arsenite and arsenate removal by in situ structural incorporation into magnetic iron(III) oxide nanoparticles, Environ. Sci. Technol. 47 (2013) 3283–3292.
[61] V.K. Sharma, Ferrate(VI) and ferrate(V) oxidation of organic compounds: Kinetics and mechanism, Coordin. Chem. Rev. 257 (2013) 495–510.
[62] N. Jaafarzadeh, F. Ghanbari, M. Ahmadi, Catalytic degradation of 2,4-dichlorophenoxyacetic acid (2,4-D) by nano-Fe_2O_3 activated peroxymonosulfate: Influential factors and mechanism determination, Chemosphere 169 (2017) 568–576.
[63] S. Nélieu, A. Lucien Kerhoas, J. Einhorn, Degradation of atrazine into ammeline by combined ozone/hydrogen peroxide treatment in water, Environ. Sci. Technol. 34 (2000) 430–437.
[64] C. Chen, S.G. Yang, Y.P. Guo, C. Sun, C.G. Gu, B. Xu, Photolytic destruction of endocrine disruptor atrazine in aqueous solution under UV irradiation: products and pathways, J. Hazard. Mater. 172 (2009) 675–684.